

A Study of the Healing-Over in the Cardiac Muscle Using Suction Electrodes

N. I. KUKUSHKIN and B. V. GUDZABIDZE

*Institute of Biological Physics, Academy of Sciences of the USSR,
142292 Pushchino, Moscow Region, USSR*

Abstract. Suction electrodes were used to investigate the phenomenon of the healing-over in preparations of rabbit, cat and dog ventricular muscles. At least two processes were shown to participate in the process of the healing-over: a rapid one (time constant approximately 1 min) and a slow one (time constant approximately 10 min). Procion Yellow dye was used to determine the size of the injured zone under the suction electrode tip. Larger tips resulted in larger zones injured. The specific resistance of the border formed during the healing over was estimated to be in the range of approx. $1 \text{ k}\Omega \cdot \text{cm}^2$, i. e. much smaller than that of the intact surface membrane.

Key words: Myocardial fibres — Healing-over — Passive electric properties — Membrane specific resistance

Introduction

The phenomenon of the healing-over in the cardiac muscle and related problems of the intercellular coupling in syncytial tissues have been the subject of an intensive investigation during the last years (for review see DeMello 1982; Loewenstein 1981). Both electrophysiological and ultrastructural methods were used to monitor the time course of the healing-over process. Significant modifications in the fine structure of gap junctions were found to occur in correlation with changes of electrophysiological parameters (Shibata and Page 1981; Dahl and Isenberg 1980) whereas the kinetics of these parameters during the healing-over has remained uncertain due to the contradictory experimental data. Thus, the injury potential measured with the method of air insulation was reported to decline within some 10—12 min (Escobar et al. 1972); the resting potential became stable within one minute after the injury (Délèze 1970) and at least three phases in the healing-over process were observed by Nishiye (1977) when the injury potential and the input resistance were estimated with the single sucrose gap technique (under normal conditions the most important exponential phase lasted approximately one minute).

Another problem concerned the quantitative evaluation of the specific resistance of the border between the normal and the injured tissue. Early attempts to approach the problem yielded only very rough estimations of this important parameter (Weidmann 1952; Délèze 1970) due to the limitations of the experimental technique.

In the present paper results of experiments with modified suction electrodes have been reported. Although the technique employed was far from being a new one, it proved to be sufficient for distinguishing two simultaneous processes participating in the healing-over (the respective time constants approximately 1 and 10 min) and for the evaluation of the specific resistance of the border between the normal and the injured tissue. Preliminary communication of the present work was published (Kukushkin and Gudzabidze 1981).

Methods

Preparations. Adult New Zealand rabbits, cats and mongrel dogs of either sex were used. Ether was used for to anesthetize cats and dogs; rabbits were killed by exsanguination. A strip (2×2 cm or less) was cut from the right ventricular wall and transferred into the perfusion chamber. Thereafter the preparation was allowed to recover for 30 min. The rate of the solution flow through the chamber was 10 ml per min. A Tyrode solution of the following composition was employed (in mmol/l): NaCl 118; KCl 4.8; $MgCl_2$ 1.0; KH_2PO_4 0.94; $NaHCO_3$ 26; glucose 10; pH 7.4 ± 0.1 . The solution was vigorously bubbled with 96% O_2 - 4% CO_2 gas mixture at 37 °C. Fig. 1 shows a scheme of the chamber with the mounted preparation.

While preparations were rather large, the properties of the tissue could not be expected to be constant in the course of an experiment (Cranefield and Greenspan 1961).

However, action potentials recorded with microelectrodes during several hours of an experiment had a fairly constant configuration, this fact suggests a good state of the superficial fibers. As for the inner layers of the tissue the possibility of the development of a hypoxic zone could not be ruled out. The influence of hypoxia on the deep fibers may have been the cause of their uncoupling (Bredikis et al. 1981; Wojtczak 1979) and of a resulting increase in the input resistance (see Fig. 2 *bottom*) observed in our experiments. The results of experiments reported below (section 2 of Results) favour the idea that hypoxia did not interfere significantly with the results of our measurements of the input resistance.

Stimulation. Surface electrodes of chlorided silver were employed for stimulation when necessary. Suction electrodes were used for the constant current injection. Each suction electrode was prepared from a glass tube with the inner surface covered by a thin layer (0.05 mm) of a highly conductive substance „contactol“ (supplied by NII GIRICOND). Because of „contactol“ the electrodes had a low proper resistance independent of temperature fluctuations. The tips of the electrodes were finely polished to obtain a good insulation of the inner solution from the bulk solution. When necessary the outer surface of the pipettes was also covered by „contactol“. The diameters of the electrode tips were approximately 0.65; 1.0 and 2.0 mm. The suction electrodes were filled with Tyrode's solution. The negative pressure applied to the suction electrodes was 2—2.2 kPa. We did not study the effects of varying this pressure. A chlorided silver plate served as the ground electrode in the bath.

Direct current pulses were delivered from the output of the isolation unit of a stimulator ESU-2. A large resistance in series with the suction electrode ensured that the current was constant and did not

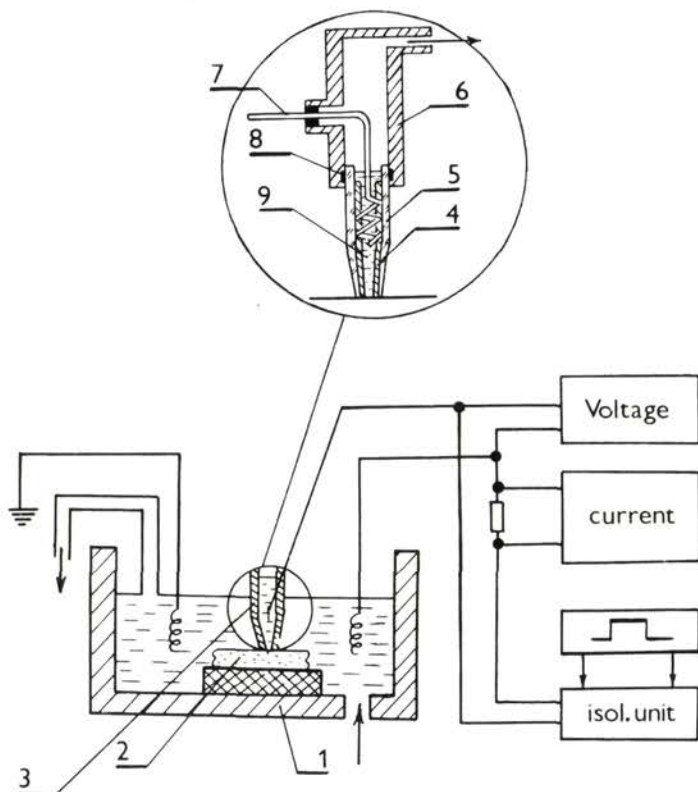


Fig. 1. Scheme of the experimental set-up. Inset: suction electrode; 1-perfusion chamber, 2-preparation, 3-suction electrode, 4-contactol layer, 5-glass pipette, 6-electrode holder, 7-silver wire, 8-vacuum ring, 9-Tyrode's solution.

depend on the proper resistance of both the suction electrode and the preparation. The amplitude of the current pulses was adjusted to induce hyperpolarization steps smaller than 4–8 mV as measured intracellularly with microelectrodes inserted close to the tip of the suction electrode. Duration of the pulses was chosen between 100 and 200 ms. The interval between the pulses was usually between 1 and several tens of seconds depending on the observed rate of the input resistance changes.

Recording. Conventional glass microelectrodes filled with 2.5 mol KCl and showing 10–20 m Ω resistance were used for the intracellular recordings of potential. The traces were displayed on the screen of an oscilloscope and photographed.

Histological methods. Suction electrodes inflicted an injury to the muscle fibres. To determine the dimensions of the zone injured under the pipette tip the dye Procion Yellow 4RS (20 mmol/l) was added to the Tyrode solution in the suction electrode before the suction was switched on. The suction was then applied for 60 min. As soon as the suction electrode had been removed, the surface of the muscle under the tip was gently smoothed and series sections (15 μ m thick) of the frozen muscle were

prepared. The sections were inspected under $\times 30$ magnification. While the intact cells have been known to be impermeable to Procion Yellow (Imanaga 1974) one could hope that a stained zone would represent the area of the tissue where the cells were injured (i. e. had a disrupted or leaky surface membrane).

Results

It may be useful to explain the rationale underlying the reported measurements of the input resistance of the suction electrodes. There is no doubt that a suction electrode would inflict a mechanical injury to the muscle fibers sucked into the tip. According to the papers cited in Introduction a healing-over process should occur on the border between the intact and damaged tissue resulting in an electrical uncoupling of the severed fibers. The idea was that the input resistance of the suction electrode might sense the changes in the passive electrical properties of the underlying tissue. An increase in the input resistance due to the uncoupling (or healing-over) could be expected.

1. Input resistance changes after the injury.

When the tip of the suction electrode was immersed into the bath containing a Tyrode solution, a finite value of input resistance, R_T , could be recorded. This value corresponded to the sum of contributions from the Tyrode solution, the ground electrode and the suction electrode itself. The input resistance increased nearly twofold as the pipette touched the surface of the muscle, and once more nearly twofold to become equal to R_0 when the suction was switched on at the "zero" moment of time.

The results are summarized in Table 1.

The initial stepwise increase from R_T to R_0 (Fig. 2) was followed by a relatively slow increment in the input resistance. In approx. 30 min a maximum input resistance, R_{max} , was achieved (see Table 1). The high value of the input resistance persisted for 1.5–2 hours and then a very slow decline began. These experimental data show, in accordance with our expectations, that the input resistance of the suction electrode began in fact to grow slowly after the injury. Curves similar to that shown in Fig. 2 were obtained in all the species studied. The results are summarized in Table 1.

The slow increase of the input resistance, R , from R_0 to R_{max} could be dissected into two exponentials fitting the equation:

$$R = R_0 + a_1(1 - \exp(-t/\tau_1)) + a_2(1 - \exp(-t/\tau_2)),$$

where a_1 and a_2 are the contributions of two exponential processes to the R growth, τ_1 and τ_2 are the respective time constants. An example of the fitting procedure is given in Fig. 3. The mean values of a_1 , a_2 , τ_1 and τ_2 measured in 55 dog ventricular muscles are shown in Table 1. The time constant of the fast exponential process (τ_1)

Table 1. The results of input resistance measurements in rabbit, cat and dog ventricular muscles, respectively. ϕ — inner diameter of the pipette tip, R_T — input resistance of the suction electrode with the tip in the solution, R_0 — input resistance measured immediately after the suction had been switched on, R_{max} — the maximum value of the input resistance, a_1 and a_2 — contributions of the fast and slow processes into the input resistance increase, τ_1 and τ_2 — the respective time constants, n — number of experiments, mean \pm SD values are shown. The results of 3 experiments performed in 3 different dog ventricular muscle preparations, where 3 exponential processes were revealed are shown below. a'_1 , a''_1 , and a_2 — the contributions of the 1st fast, 2nd fast, and the slow process respectively into the input resistance increase, τ'_1 , τ''_1 and τ_2 — the respective time constants of the processes a'_1 , a''_1 , a_2 respectively.

Ventricle preparation	ϕ [mm]	R_T [k Ω]	R_0 [k Ω]	R_{max} [k Ω]	a_1 [k Ω]	a_2 [k Ω]	τ_1 [min]	τ_2 [min]	n		
Dog	≈ 0.65	1.95 ± 0.20	5.64 ± 0.35	11.51 ± 0.39	4.52 ± 0.19	1.62 ± 0.17	0.75 ± 0.06	9.2 ± 0.8	14		
	≈ 1	0.84 ± 0.02	2.55 ± 0.09	5.22 ± 0.19	1.95 ± 0.12	0.80 ± 0.08	0.85 ± 0.05	12.3 ± 0.7	19		
	≈ 2	0.40 ± 0.03	1.51 ± 0.07	2.88 ± 0.10	0.87 ± 0.07	0.69 ± 0.08	0.88 ± 0.05	10.4 ± 0.6	22		
Cat	≈ 1	1.23 ± 0.10	5.44 ± 0.60	12.7 ± 1.0	2.26 ± 0.24	4.97 ± 0.74	—	11.3 ± 1.5	12		
	≈ 2	0.47 ± 0.03	1.83 ± 0.09	4.02 ± 0.23	0.75 ± 0.05	1.44 ± 0.26	—	9.6 ± 2.6	3		
Rabbit	≈ 1	1.20 ± 0.04	6.1 ± 0.2	15.5 ± 0.6	2.80 ± 0.32	6.60 ± 0.45	—	11.7 ± 0.6	36		
	≈ 2	0.43 ± 0.04	1.70 ± 0.18	4.03 ± 0.34	0.61 ± 0.13	1.73 ± 0.19	—	9.1 ± 0.9	11		
	ϕ [mm]	R_0 [k Ω]	R_T [k Ω]	R_{max} [k Ω]	a'_1 [k Ω]	a''_1 [k Ω]	a_2 [k Ω]	τ'_1 [min]	τ''_1 [min]	τ_2 [min]	n
Dog	≈ 0.65	1.50 ± 0.01	4.67 ± 0.33	10.4 ± 0.1	2.03 ± 0.11	2.68 ± 0.28	1.03 ± 0.05	0.35 ± 0.02	1.38 ± 0.09	7.78 ± 0.45	3

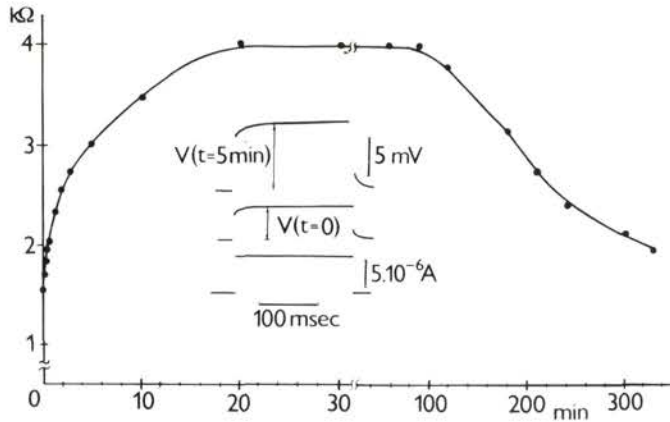


Fig. 2. Time dependence of the input resistance of the suction electrode. The inner diameter of the electrode tip was 1.910 mm. R_0 was 1.53 k Ω , R_{max} was 4.07 k Ω . Inset: an example recording ($R = V/I$, V and I are stationary values of the potential and current respectively).

was not measured in cat and rabbit ventricular muscles; in these preparations a_1 , a_2 and τ_2 were only determined. The time constants of the slow process were in good agreement in all species studied (close to 10 min) though the contributions of the slow process to the total increment of the input resistance were different in different species. In dog ventricle, some 25–35% of the total R increment were due to the slow exponential process, and in cat and rabbit ventricles it made up to nearly 70% of the R increment.

It is interesting that the pipettes with different tip diameters displayed different absolute values of the input resistance but they yielded generally similar parameters of the two exponential processes (a_1/a_2 , τ_1 , τ_2) for each species. Moreover, the values of τ_2 were similar in all species and when measured with different pipettes. This observation suggests that the kinetic behaviour of the input resistance during the first 30 min after the injury probably reflected some intrinsic properties of the injured tissue.

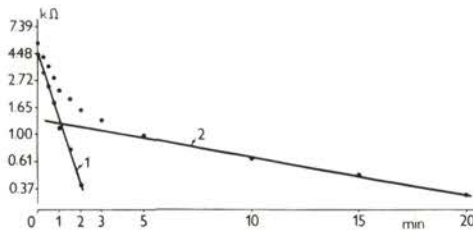


Fig. 3. Logarithmic plot of the input resistance dependence on time. Points represent the experimental results, the lines were drawn by eye. Dog ventricular muscle.

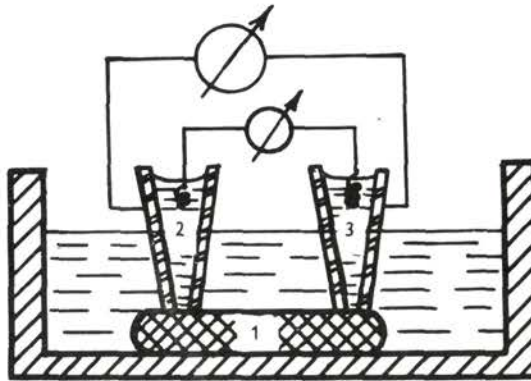


Fig. 4. Scheme of the experimental set-up to measure the leakage current under the pipette tip in the cat ventricular muscle. 1-preparation, 2,3-suction electrodes. Both the inner and outer surface of pipettes were covered by contactol.

In 3 preparations of the dog ventricular muscle three exponential processes could be distinguished. The slowest exponential process had the rate similar to that of the slow one revealed when the two exponentials were used for approximation. The other two exponentials had time constants comparable with τ_1 of the rapid process described above (0.3 and 1.4 min respectively).

These results show that the input resistance of the suction electrode not only senses the probable uncoupling that occurs in the injured zone but also permits to distinguish at least two exponential processes in this phenomenon.

2. Evaluation of the insulation of the suction electrode tip.

It is clear that a large leakage current may exert an important and hardly predictable influence on the input resistance. Such a current may flow from the inner side of the pipette to the bulk solution through a poorly sealed contact between the pipette tip and the surface of the muscle. The purpose of the experiments described in this section was to evaluate the leakage current. For this purpose an isotonic sucrose solution was introduced into the bath. If the leakage current were large, this solution would increase considerably the input resistance of the suction electrode, due to the reduction of the leakage current flowing through the bathing solution. To make the input resistance of the suction electrode less dependent on the composition of the bathing fluid, a second suction electrode was employed instead of a ground silver plate. The experimental arrangement is shown in Fig. 4. Both electrodes had highly conductive layers on the inner and outer surfaces of their tips. Consequently two parameters could be measured: the resistance between the outer surfaces and that between the inner surfaces of their

tips. The distance between the outer surfaces of the electrode tips ranged from 0.8 to 1.3 mm, the diameter of the tips was approximately 1 mm.

Measurements were performed after more than 30 min of suction, i. e. during the plateau phase of the input resistance changes (see Fig. 2). With Tyrode's solution in the bath, the resistance between the inner surfaces of the suction electrodes was approximately double the input resistance of a single electrode. Then the sucrose solution was introduced for one minute (it took several seconds to change the solution). In five preparations studied, a considerable increase in the resistance between the outer surfaces of the electrodes (more than 30-fold) was observed; at the same time only an insignificant increase in the resistance between the inner surfaces of the electrodes was found (less than 0.04 of the initial value). The result is clearly incompatible with the notion of the poor insulation of the suction electrode tip: in case of a poor insulation the sucrose solution should have caused a great increase in the input resistance (due to the leakage current reduction). The results of measurements are summarized in Table 2. They show that the insulation of the pipette tip during the plateau phase of the input resistance changes may be considered to be quite perfect.

Further experiments showed that this conclusion could not be extended to the late (after 2—3 hours of suction) phase of the slow decline of the input resistance. The experiment with a brief sucrose introduction in the bath was repeated at the time when the input resistance of a single suction electrode in a conventional experiment (like in Fig. 2) began declining. Now introduction of the sucrose caused a considerable enhancement of the resistance between the inner surfaces of the electrodes. The enhancement became increasingly pronounced with time as the slow decline of the input resistance was progressing. The sucrose restored the high value of the input resistance of the system of two suction electrodes. Table 2 shows the results.

These results throw light on the cause of the slow decline in the input resistance after a few hours of suction. They show that in the course of the experiment a very slow deterioration of the insulation of the pipette tip took place. This deterioration of the insulation was probably the major cause of the very slow decline in the suction electrode input resistance. The causes of the deterioration of insulation were not examined. The early changes in the single suction electrode input resistance occurring within 30 min may tentatively be suggested to be determined by factors other than the leakage current.

Experiments reported in the following two sections were performed to provide data necessary for a quantitative evaluation of the specific resistance of the border between the normal and the injured zone. Based on these data and on several assumptions, the calculations of the specific resistance were done (section 5).

Table 2. The input resistance of the tissue (R_{is}) as measured between the inner surfaces of two suction electrodes (Fig. 4) (dog ventricular muscle). t — time since suction has been switched on, R_{is}^n — in Tyrode, R_{is}^s — in sucrose, L — the minimum distance between the outer edges of the pipettes.

t [min]	R_{is}^n [k Ω]	R_{is}^s [k Ω]	$(R_{is}^s - R_{is}^n)/R_{is}^n$ [%]	L [mm]
55	9.42	9.8	3.9	0.85
60	10.85	11.5	5.6	1.0
60	8.7	9.03	3.7	1.0
65	9.42	9.67	2.7	1.3
70	8.5	8.7	2.1	0.9
132	9.42	9.67	2.7	1.3
204	8.80	10.3	17	0.85
258	6.84	11.2	64	0.9
315	6.67	11.1	66	1.0
426	4.1	8.5	108	1.0

3. Size of the injured zone.

Besides the general interest, the size of the injured zone is important for our calculations. The procedure employed for the visualization of the injured zone was described in Methods. The diameters of the electrode tips were approximately 0.65; 1.0 and 2.0 mm.

A distinct boundary between the stained (presumably injured) and the unstained (supposedly normal) zones was observed. The surface of this boundary could be approximately described as that of a half of a rotation ellipsoid. In our calculations, the small axis was taken to represent the depth of the injury zone, and the greater one the radius of the stained zone as seen on the surface of the muscle. The results are presented in Table 3. The main conclusion is almost trivial: the tips of greater diameter caused larger injury zones.

4. Measurements of the portion of the current injected intracellularly through the suction electrodes.

It is shown in Appendix that to evaluate the portion of the current injected intracellularly by suction electrodes dV_i/dX and dV_e/dX must be determined (V_i and V_e are intra- and extracellular potentials induced by the current flow through the tissue, and X is the distance from the suction electrode along an arbitrary axis). Moreover, it is necessary to measure dV_i/dX and dV_e/dX values in the close vicinity of the suction electrode.

Table 3. Dimensions of the injured zone for different electrode tip diameters. ϕ — the inner diameter of the pipette tip; H — the depth of the injured (stained) zone; D — the diameter of the stained zone on the surface of the muscle; S_{inj} — the surface of the injured zone calculated on the assumption that the injured zone is a half of rotation ellipsoid; n — number of experiments, mean \pm SD values are shown.

ϕ [mm]	D [mm]	H [mm]	S_{inj} [cm ² $\times 10^{-3}$]	n
0.65	0.76 \pm 0.02	0.14 \pm 0.01	5.61 \pm 0.23	4
1	1.2 \pm 0.03	0.24 \pm 0.01	14.2 \pm 0.7	5
2	2.2 \pm 0.4	0.38 \pm 0.01	44.0 \pm 1.4	4

Microelectrodes were employed to measure V_i and V_e (electrotonic decline in the intracellular and extracellular space respectively) in different directions chosen routinely to be parallel or orthogonal to the fibers. The direction of the fibres was determined by eye as seen on the surface of the preparation. The microelectrodes were impaled into the first two layers of cells on the surface of the muscle to record V_i ; to record V_e , they were gently pulled backwards until the membrane potential disappeared as soon as the microelectrode presumably entered the extracellular space. Measurements started 30 min after the suction had been switched on when the input resistance of the suction electrode had become stabilized. The experiment was terminated before the 90th minute, i. e. safely before the slow downward creep of the input resistance caused by the growing leakage current began. An example of experimental recordings is shown in Fig. 5.

The potential gradients were calculated according to the equations:

$$(dV_i/dX)_{X=X_0} = (V_i(X_0 + \Delta X) - V_i(X_0))/\Delta X = \Delta V_i/\Delta X,$$

$$(dV_e/dX)_{X=X_0} = (V_e(X_0 + \Delta X) - V_e(X_0))/\Delta X = \Delta V_e/\Delta X,$$

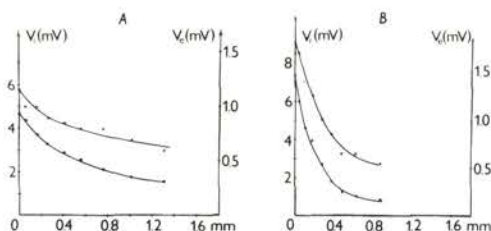


Fig. 5. Decline of the electrotonic potential on the endocardial side of the dog right ventricular wall preparation. A—in parallel to the fibers, B—in the transverse direction, crosses: the extracellular potential (V_e); circles — the intracellular potential (V_i). The point $X=0$ was chosen at the outer edge of the suction electrode tip (tip diameter 2 mm, tip wall thickness 0.250 mm).

Table 4. Distribution of the injected current between the intra and extracellular spaces. ϕ — the inner diameter of the pipette tip; $dV_i/dX_{x=0}$ and $dV_e/dX_{x=0}$ — gradients of the electrotonic decline close to the suction electrode tip determined according to the equations given in section 4 of Results for the intracellular and extracellular space, respectively; $(dI_i/dI_e)_{x=0}$ — relation of the current injected intracellularly to that injected extracellularly calculated according to eqs 1 and 2 (Appendix).

ϕ [mm]	Along the fibres			Transversedirection			„Integral“ (all directions)		
	0.6	1.0	2.0	0.6	1.0	2.0	0.6	1.0	2.0
$(dV_i/dX)_{x=0}$ (mV/mm)	18.1 ± 2.1 n = 11	22.6 ± 3.9 n = 8	16.1 ± 2.8 n = 10	16.1 ± 2.2 n = 9	13.4 ± 5.6 n = 7	13.8 ± 3.2 n = 10	—	—	—
$(dV_e/dX)_{x=0}$ (mV/mm)	0.75 ± 0.08 n = 11	1.22 ± 0.22 n = 8	1.02 ± 0.34 n = 10	1.54 ± 0.23 n = 9	1.41 ± 0.30 n = 7	1.85 ± 0.37 n = 10	—	—	—
$(dI_i/dI_e)_{x=0}$	8.8 ± 1.4 n = 11	8.2 ± 1.3 n = 8	6.8 ± 1.3 n = 10	1.55 ± 0.29 n = 9	1.11 ± 0.33 n = 7	0.97 ± 0.22 n = 10	5.2	4.7	3.9

where X_0 was usually 0.01–0.02 mm from the wall of the pipette tip and ΔX was chosen to be 0.1 mm. Then the portion of the current injected intracellularly was determined according to eqs. 1 and 2 (see Appendix). The results of measurements and calculations are summarized in Table 4.

Table 4 shows that the portion of the current injected intracellularly depends on the direction. In parallel to fibres, the bulk of the current was injected intracellularly, while in the transverse direction (at the right angle to the fibres) a considerable portion of the current was flowing into the extracellular space. The portion of the current injected intracellularly in any of the two directions was generally smaller for greater diameters of the pipette tips.

In the following section, we shall need an integral value of the portion of the current injected intracellularly in all directions. This parameter was calculated as the mean of the portions of the current injected intracellularly in parallel to the fibers and in the transverse direction. The results are shown in Table 4. The employed rough approximation yields a reduced value of the integral portion of the current injected intracellularly in all directions because most of the injected current flows in parallel to the fibres and not in the transverse direction (Clerc 1976).

5. Estimation of the specific resistance of the injured intact zone border.

We attempted to deduce some quantitative characteristics of the injured zone from the data on the input resistance changes. The calculations necessarily rely on several assumptions: (1) the increase in the input resistance from R_0 to R_{\max} is due to the formation of a border between the intact and the injured zone. An analysis of this assumption is presented in Discussion.

If the leakage current flowing under the tip of the suction electrode straight into the bathing solution is neglected, according to the first assumption the lower estimation of the total resistance of the new border may be written as

$$R_b^{\min} = R_{\max} - R_0 .$$

This estimation is likely not very far from being exact because the leakage current has been shown to be comparatively small (see Results, section 2).

The total resistance can be converted into the specific one using the estimations of the area of the border presented in Table 3:

$$r_b^{\min} = R_b^{\min} \times S_{inj} .$$

The values of r_b^{\min} obtained for different diameters of electrode tips are shown in Table 5. Most of the r_b^{\min} values measured with different tip diameters are in a reasonable agreement in all species studied as it could be expected if the assumption (1) was true. Significant deviations were observed only with large

pipettes (tip diameter of 2 mm) employed in dog ventricular muscle. Nevertheless, pipettes with smaller tips gave consistent results also in this preparation; based on this it could be concluded that the large pipettes were inadequate for measurements of r_b^{\min} in dog ventricular muscles.

It is generally believed that the electrical uncoupling on the border of the injured zone occurs as a result of a modification of the intercellular contacts (DeMello 1982). The second assumption concerns this concept: (2) the new border forms on the intracellular pathways only. In other words, the new border is supposed to form on the intercellular contacts. Consequently, the estimation procedure for the specific resistance of the border should undergo modification.

The input resistance of the tissue may be split into the input resistance of the extracellular pathways, R_e , and the input resistance of the intracellular pathways, R_i . The tissue input resistance at $t=0$ is obviously

$$R_0^{\text{tis}} = R_e R_i / (R_e + R_i) .$$

It should be noted that the distributed membrane resistance is incorporated in R_e and R_i (R_e and R_i are regarded as the input resistances of a complex distributed circuit with a generally unknown geometry and a grounded output).

When the border has formed the tissue input resistance becomes equal to

$$R_{\max}^{\text{tis}} = R_e R'_i / (R_e + R'_i) ,$$

where R'_i is the new input resistance of the intracellular pathways modified by the formation of the border with the proper resistance R_b :

$$R'_i = R_i + R_b .$$

The values of R_{\max}^{tis} and R_0^{tis} can be derived from the experimentally obtained parameters

$$R_0^{\text{tis}} = R_0 - R_T ,$$

$$R_{\max}^{\text{tis}} = R_{\max} - R_T .$$

Simple arithmetics yield the resistance of the border on the intracellular pathways:

$$R_b = R_{\max}^{\text{tis}} (R_0^{\text{tis}} - R_{\max}^{\text{tis}}) (k + 1)^2 / k (R_0 - (k + 1) R_{\max}^{\text{tis}}) ,$$

where

$$k = R_e / R'_i .$$

The parameter k represents the distribution of the injected current between the extracellular and the intracellular pathways following the border formation. It was approximately determined in Section 4 of Results (Table 4) as the integral portion

of the current injected intracellularly. Using the results from Tables 1 and 4 the R_b values shown in Table 5 can be calculated. These are the values of the border resistance if the border is supposed to form on the intracellular pathways only.

It is also possible to estimate the specific resistance of the border on the intracellular pathways. In estimating this specific resistance the sinuosity factor of 9 suggested by Page and MacCallister (1973) for the surface of intercalated discs cannot be neglected. Hence the specific resistance of the new border may be written as

$$r_b = R_b \cdot 9 S_b .$$

It has already been shown that at least two exponential processes participate in the slow growth of the input resistance. Thus it may be interesting to know the contributions of the two processes into the specific resistance of the border. The contribution of the slow process is obviously proportional to

$$\eta = a_2 / (a_1 + a_2) ,$$

and the contribution of the rapid process is proportional to $(1 - \eta)$ (a_1 and a_2 see Table 1). The contributions of the two processes into the specific resistance of the border, r_{b1} and r_{b2} , are shown in Table 5. They are obviously different in different species.

In conclusion, it may be noted that all our estimations of the specific resistance of the new border give clearly smaller values than those reported for the specific resistance of the intact surface membrane ($10 \text{ k}\Omega \times \text{cm}^2$ according to Weidmann 1970).

Discussion

Two major results have been presented: (1) the injury-associated growth of the suction electrode input resistance can be split up into two exponential processes; (2) the specific resistance of the presumable border between the normal and the injured zone of the muscle is estimated to be much smaller than the specific resistance of the intact surface membrane.

The adequacy of the method.

It is important to know to what extent the results of the input resistance measurements represented the intrinsic properties of the injured tissue, and to what degree the properties of the suction electrodes. One approach to this complex problem may consist in a comparison of the results obtained with suction electrodes of different tip diameters. If the input resistance changes did indeed reflect

Table 5. Total and specific resistances of the border. R_0^{is} — proper tissue input resistance; R_{max}^{is} — maximum tissue input resistance; R_b — total resistance of the new border; R_b^{min} — lower estimation of the total resistance of the new border; r_{b1} and r_{b2} — specific resistances of the new border due to the fast and slow processes respectively; $r_b = R_b \times 9S_b$, where S_b is the surface area of the stained zone and 9 is the sinuosity factor; r_{b1}^{min} and r_{b2}^{min} — lower estimations of the specific resistances of the border due to the fast and slow processes respectively; $r_b^{min} = R_b^{min} \times S_b$; n — number of experiments, mean \pm SD values are presented; ϕ — the suction electrode diameter.

Ventricle preparation	n	ϕ [mm]	R_0^{is} [k Ω]	R_{max}^{is} [k Ω]	R_b^{min} [k Ω]	R_b [k Ω]	r_{b1}^{min} [$\Omega \cdot \text{cm}^2$]	r_{b2}^{min} [$\Omega \cdot \text{cm}^2$]	r_b^{min} [$\Omega \cdot \text{cm}^2$]	r_b [$\Omega \cdot \text{cm}^2$]	r_{b1} [$\Omega \cdot \text{cm}^2$]	r_{b2} [$\Omega \cdot \text{cm}^2$]
Dog	14	≈ 0.65	3.70 \pm 0.24	9.50 \pm 0.36	5.80 \pm 0.20	7.38 \pm 0.42	24.5 \pm 1.0	9 \pm 1	33.3 \pm 2.2	0.38 \pm 0.03	0.28 \pm 0.02	0.103 \pm 0.011
	19	≈ 1	1.71 \pm 0.09	4.33 \pm 0.20	2.67 \pm 0.15	3.41 \pm 0.36	26.7 \pm 2.2	13 \pm 1	38.8 \pm 3.2	0.44 \pm 0.04	0.30 \pm 0.03	0.138 \pm 0.020
	22	≈ 2	1.11 \pm 0.06	2.52 \pm 0.11	1.41 \pm 0.08	1.95 \pm 0.18	34.5 \pm 2.2	27.2 \pm 3.0	61.1 \pm 4.5	0.74 \pm 0.07	0.43 \pm 0.04	0.31 \pm 0.04
Cat	12	≈ 1	4.20 \pm 0.52	11.50 \pm 0.98	7.13 \pm 0.73	9.46 \pm 1.21	32.2 \pm 3.2	65.5 \pm 10.0	97.8 \pm 11.2	1.17 \pm 0.16	0.38 \pm 0.04	0.78 \pm 0.13
	3	≈ 2	1.37 \pm 0.11	3.55 \pm 0.20	2.19 \pm 0.29	2.97 \pm 0.90	32.2 \pm 2.4	61.0 \pm 11.1	92.4 \pm 11.2	1.12 \pm 0.31	0.39 \pm 0.13	0.73 \pm 0.27
Rabbit	36	≈ 1	4.90 \pm 0.19	14.35 \pm 0.62	9.40 \pm 0.54	12.19 \pm 1.27	48.9 \pm 4.5	86.8 \pm 5.5	135.5 \pm 9.1	1.58 \pm 0.16	0.57 \pm 0.06	1.01 \pm 0.13
	11	≈ 2	1.27 \pm 0.16	3.60 \pm 0.33	2.34 \pm 0.21	3.15 \pm 0.42	27.8 \pm 6.7	75.6 \pm 10.0	103.5 \pm 15.1	1.25 \pm 0.23	0.34 \pm 0.10	0.91 \pm 0.19

processes that occurred in the injured muscle, some parameters independent on the diameter of the electrode tip may be found. Such parameters were found indeed; they included the kinetic characteristics of the input resistance growth and the specific resistance of the presumable border between the normal and the injured zone. The relative independence of these parameters on the size of the electrode tip permits the suggestion that they represented the real properties of the injured tissue.

The latter statement has of course certain limitations. It was mentioned in Results that when pipettes with large tips (2 mm in diameter) were applied to the dog ventricular muscle, a deviation of the value of the estimated specific resistance of the border was observed. At the same time smaller pipettes gave consistent results. Hence it can be seen that suction electrodes with large tip diameters do not give adequate results when applied to the dog ventricular muscle. We shall show that this inadequacy is due to the development of a hypoxic zone.

Another important problem associated with the adequacy of the method is the evaluation of the insulation under the tip. Many of the calculations presented in Results rely on the assumption that the leakage current flowing under the tip directly into the surrounding solution is small. This assumption could be confirmed in experiments in which sucrose was introduced into the chamber.

What was the cause of the input resistance increase?

We believe that there are two possible causes of the input resistance increment after the injury. First, the increase in the input resistance of the suction electrode may reflect the healing-over process after the mechanical injury, inflicted by the pipette tip at the moment when the suction was switched on. It is clear that the "sealing" of the injured zone may have increased the input resistance of the suction electrode. Second, the uncoupling of the cells due to the formation of a hypoxic zone under the pipette tip may have contributed to the increase in the input resistance. The latter does not seem plausible in view of the following. Pipettes of different tip diameters most probably create different hypoxic zones and the resistance of the zones depends on their dimensions. It is clear that the resistance of the hypoxic zone is inversely proportional to the first degree of its effective diameter, and the latter can be reasonably regarded as proportional to the diameter of the electrode tip. Hence the resistance of the hypoxic zone should expectedly be inversely proportional to the first degree of the tip diameter of the pipette. However, the computations show that the total resistance increment after the injury is inversely proportional to the surface area of the injured zone. The only exception to this rule was observed when large pipettes were employed in dog ventricular muscle. In this case, hypoxia must have been important.

The observation that the total increase in the input resistance after the injury

was inversely proportional to the surface area of the injured zone is in agreement with the first alternative (i.e. that the healing-over accounted for the increase in the input resistance). This is so because in contrast to hypoxia healing-over is supposed to occur not in volume but along the boundary of the injured zone. It is therefore possible to suggest that the healing-over process was probably the major cause of the increase in the suction electrode input resistance after the injury.

Kinetics of the input resistance increase after the injury.

While it is supposed that the increase in the input resistance was due mainly to a process similar to the healing-over, it may be interesting to see whether the results obtained in experiments with suction electrodes correlate with those obtained with other methods.

Electron microscopy revealed two kinds of modifications in the ultrastructure of nexuses after the injury: one of them (increase in the so-called P-face particle diameter) was relatively rapid (it took less than a minute) and the other one was slower (in the range of 30 min) and concerned the center-to-center distances of P-face particles (Shibata and Page 1981). This finding is in agreement with our result concerning the kinetics of the two exponential processes participating in the input resistance increase (time constants approximately 1 and 10 min respectively).

The results of electrophysiological observations usually reveal either a rapid (Délèze 1970; Ochi and Nishiye 1973) or a slow process (Escobar et al. 1972). Nishiye (1977) reported that the input resistance of the sucrose gap and the injury potential as measured with the sucrose gap technique in the guinea-pig papillary muscle drifted in the majority of cases slowly to a stable level within approximately 1 minute after the injury. Nevertheless the author noted that a slower phase of the changes in the measured parameters could be occasionally discerned in some preparations. These findings are also not contradictory to our results, though the reason for the irregular observation of the slow phase using the sucrose gap technique remained unclear. It may be suggested that the rapid process ensured a sufficient increase in the resistance of the border between the normal and the injured zone to restore the normal resting potential in intact cells. Then it becomes clear why the measurements of the injury potential could not sense any further changes in the border resistance. This reasoning leaves however unclear the causes of the failure to detect the slow phase regularly by means of the input resistance measurements with the sucrose gap technique in similar experiments. This failure may have been due to the large distance between the sucrose gap and the injured zone.

Our results nevertheless support the viewpoint that the healing-over process occurs in two phases, a rapid and a slow one.

What is the mechanism underlying the increase in the input resistance?

If we assume that healing-over is the underlying mechanism of the increase in the input resistance it is possible to draw a conclusion that calcium ions play an important role in it (DeMello 1972, 1975). This suggestion is consistent with the fact that the increase in the suction electrode resistance was greatly suppressed when EGTA was added into the inner solution of the pipette (not documented).

Estimations of the specific resistance of the presumable border between the normal and the injured tissue.

Weidmann (1952) and Délèze (1970) attempted to estimate the specific resistance of the border between the intact and the injured cells in the cardiac muscle. Both authors agreed that the new border had a high resistance comparable with the normal membrane resistance. Their results did not permit a more direct estimation.

The results of the present paper suggest that the specific resistance of the new border that forms after the injury (r_b) is close to $1000 \Omega \times \text{cm}^2$ for the species studied. This value is considerably smaller than the specific resistance of the intact surface membrane ($10 \text{ k} \Omega \times \text{cm}^2$) for sheep ventricular fibres (Weidmann 1970). It is important that this conclusion is valid regardless of the possible interference of hypoxia since the latter could only increase the r_b value. Another interesting aspect is that this low value of r_b is still much greater than the normal specific resistance of the intercellular contacts ($1 \Omega \times \text{cm}^2$; DeMello 1982).

When a microelectrode was used to record action and resting potentials at different distances from the suction electrode, reduced values of the parameters could be observed close to the pipette tip (an example is shown in Fig. 6). This fact

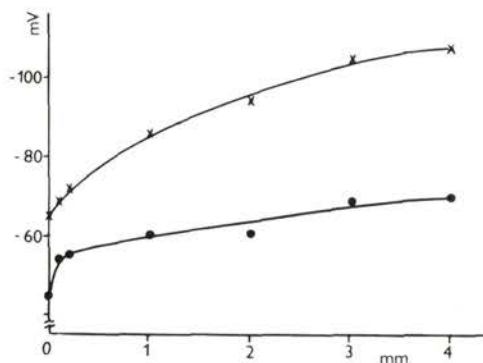


Fig. 6. Dependence of the resting (circles) and the action potential amplitudes (crosses) on the distance from the suction electrode in dog ventricular muscle. The point $X = 0$ was again at the outer edge of the tip (diameter 2 mm, wall thickness 0.250 mm).

is very difficult to explain unless the existence of a hypoxic zone under and close to the tip is supposed. It may be therefore supposed that intercellular contacts in this zone have a high resistance. Nevertheless the space constant was found to be close to normal, even in the vicinity of the tip, showing that the contacts in the zone were relatively good. This conclusion is true for the surface fibres only, with no regard to the situation in deeper layers of the muscle.

Appendix

It is beyond the scope of our possibilities to measure directly the portion of the current injected intracellularly through a suction electrode. However it is possible to determine locally the relation of the current flowing intracellularly to that flowing extracellularly. If such local measurements are performed in a close vicinity of the suction electrode tip they may permit to evaluate the portion of the current injected intracellularly.

The intra- and extracellular potentials induced by the current injected through a suction electrode are generally complex functions of coordinates ($V_i[x, y, z]$ and $V_e[x, y, z]$ respectively) because of the complex tissue geometry and the anisotropy of the specific resistance. It is however possible to regard a volume sufficiently small to avoid some complications of anisotropy and to assume that the specific resistances within this volume are constant. Another assumption is that this volume is still large enough as compared with a single cell, and hence the media (tissue) may be considered as homogeneous in this volume. Then it becomes possible to estimate the relation of the currents flowing extra- and intracellularly through an arbitrary small flat surface in this volume. When the volume is chosen close to the suction electrode the obtained relation gives the solution of the problem.

It is convenient to determine the position of the microelectrode in relation to the suction electrode. For this reason we chose an arbitrary axis, OX , passing through the centre of the suction electrode tip and then we regard two points X and $X + dX$ surrounded by a small volume, Ω , on this axis (Fig. 7). The small volume should satisfy the following conditions:

- (1) the equipotential surfaces $V_i(X)$ and $V_i(X + dX)$ are parallel and virtually flat in Ω ;
- (2) similarly $V_e(X)$ and $V_e(X + dX)$ are also virtually parallel and flat in Ω ;
- (3) the membrane current is negligibly small as compared with intra- and extracellular currents in Ω ;
- (4) in Ω the intra- and extracellular specific resistances may be considered as constant.

Then a small flat surface dS_n can be chosen in Ω (dS_n orthogonal to OX) so that the projections of this surface on the surfaces $V_i(X)$ and $V_i(X + dX)$ also lie in Ω . The intracellular current flowing across this surface

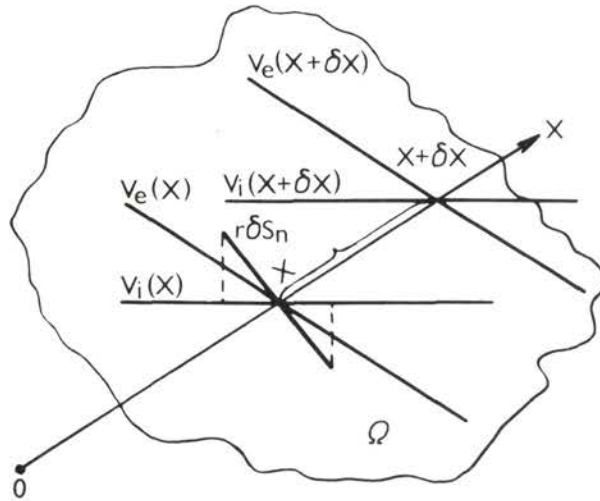


Fig. 7. Derivation scheme of eqs. 1 and 2 (Appendix), OX is an arbitrary axis that may pass through the centre of the pipette tip, dS_n is a small flat surface orthogonal to OX . $V_e(X)$; $V_i(X+dX)$; $V_e(X)$; $V_e(X+dX)$ are the equipotential surfaces.

$$dI_i(X) = (V_i(X) - V_i(X+dX)) / \bar{\rho}_i(X) dX \cos \alpha dS_n^{-1} \cos^{-1} \alpha = (dS_n / \bar{\rho}_i(X)) (dV_i/dX),$$

where $\bar{\rho}_i(X)$ is the specific resistance of the intracellular space to the current flowing in the direction of the grad $V_i(X)$, α is the angle between the OX axis and the surface $V_i(X)$.

Similarly, for the extracellular current flowing across dS_n can be written

$$dI_e(X) = (dS_n / \bar{\rho}_e(X)) (dV_e/dX).$$

Hence the relation of the currents flowing intra- and extracellularly through the dS_n is

$$dI_i(X) / dI_e(X) = (\bar{\rho}_e(X) / \bar{\rho}_i(X)) (dV_i/dX) / (dV_e/dX).$$

The values of dV_i/dX and dV_e/dX may be estimated from experimental measurements. The values of $\bar{\rho}_i(X)$ and $\bar{\rho}_e(X)$ vary throughout the preparation and cannot be measured directly. Nevertheless, literary data may be used to estimate these values roughly. When the fibres are parallel within the volume Ω , $\bar{\rho}_e(X)$ must be identical with the specific resistance $\rho_e(X)$ of the liquid filling the extracellular space. In other words, $\bar{\rho}_e(X)$ is the specific resistance of the tissue for the current flowing extracellularly taking in account that the extracellular space occupies only a part of the total tissue volume.

If the fibres are parallel in the volume Ω the relation $n = \rho_c(X)/\bar{\rho}_c(X)$ must coincide with the relation of the area occupied by the extracellular space in the tissue section by dS_n to the total area of dS_n . The same holds for the intracellular space: $\rho_i(X)/\bar{\rho}_i(X) = m = \text{const}$ where m is the portion of the area occupied by the intracellular space on the section of the tissue by the surface dS_n . Now the relation of the currents may be rewritten as

$$dI_i/dI_e = (m/n)(\rho_c(X)/\rho_i(X))((dD_i/dX)/(dV_e/dX)).$$

The value of m/n was estimated to be approximately 3 (Page 1962). The mean values of ρ_c and ρ_i for two orthogonal directions have been reported, in parallel to the fibres and in the transverse direction (Clerc 1976). Using these values of ρ_c and ρ_i measured in the calf ventricular muscle the following result is obtained:

(a) in parallel to the fibres

$$(1) \quad (dI_i/dI_e) = 0.36((dV_i/dX)/(dV_e/dX)) ;$$

(b) in the transverse direction

$$(2) \quad (dI_i/dI_e) = 0.11((dV_i/dX)/(dV_e/dX)) .$$

References

- Bredikis J. J., Bukauskas F. F., Veteikis R. P. (1981): Decreased intracellular coupling after prolonged rapid stimulation in rabbit atrial muscle. *Circ. Res.* **49**, 815—820
- Clerc L. (1976): Directional differences of impulse spread in trabecular muscle from mammalian heart. *J. Physiol. (London)* **255**, 335—346
- Cranefield P. F., Greenspan K. (1961): The rate of oxygen uptake of quiescent cardiac muscle. *J. Gen. Physiol.* **44**, 235—247
- Dahl G., Isenberg G. (1980): Decoupling of heart muscle cells: correlation with increased cytoplasmic calcium activity and with changes of nexus ultrastructure. *J. Membrane Biol.* **53**, 63—77
- Dèlèze J. (1970): The recovery of resting potential and input resistance in sheep heart injured by knife or laser. *J. Physiol. (London)* **208**, 547—562
- DeMello W. C. (1972): The healing-over process in cardiac and other muscle fibers. In: *Electrical Phenomena in the Heart* (Ed. W. C. DeMello) pp. 323—351, Academic Press, New York, London, Toronto, Sidney, San Francisco
- DeMello W. C. (1975): Effect of intracellular injection of calcium and strontium on cell communication in heart. *J. Physiol. (London)* **250**, 231—247
- DeMello W. C. (1982): Cell-to-cell communication in heart and other tissues. *Progr. Biophys. Mol. Biol.* **39**, 147—183
- Escobar J., DeMello W. C., Perez B. (1972): Healing-over and muscle contraction in toad hearts. *Circ. Res.* **31**, 389—396
- Imanaga I. (1974): Cell-to-cell diffusion of Procion Yellow in sheep and calf Purkinje fibres. *J. Membrane Biol.* **16**, 381—388
- Kukushkin N. I., Gudzabidze B. V. (1981): Healing-over in cardiac ventricular muscle. In: VII International Biophysics Congress (Abstracts) p. 257, Mexico City
- Loewenstein W. R. (1981): Junctional intercellular communication: the cell-to-cell membrane channel. *Physiol. Rev.* **61**, 829—914
- Nishiye H. (1977): The mechanism of Ca^{2+} action on the healing-over process in mammalian cardiac muscle: A kinetic analysis. *Jpn. J. Physiol.* **27**, 451—466

- Ochi R., Nishiye H. (1973): Temperature dependence of the healing-over in mammalian cardiac muscle. *Proc. Jpn. Acad. Sci.* **49**, 372—375
- Page E. (1962): Cat heart muscle in vitro. III. The extracellular space. *J. Gen. Physiol.* **46**, 201—213
- Page E., MacCallister L. F. (1973): Studies on the intercalated disk of rat ventricular myocardial cells. *J. Ultrastruct. Res.* **43**, 388—411
- Shibata Y., Page E. (1981): Gap junctional structure in intact and cut sheep cardiac Purkinje fibers: A freeze-fracture study of Ca^{2+} -induced resealing. *J. Ultrastruct. Res.* **75**, 195—205
- Weidmann S. (1952): The electrical constants of Purkinje fibers. *J. Physiol. (London)* **118**, 348—360
- Weidmann S. (1970): Electrical constants of trabecular muscle from mammalian heart. *J. Physiol. (London)* **210**, 1041—1054
- Wojtczak J. (1979). Contractures and increase in interal longitudinal resistance induced by hypoxia. *Circ. Res.*, **44**, 88—95

Received March 11, 1983 / Accepted April 24, 1983